VSP Journal of Adhesion Science and Technology 22 (2008) 687–698
Journal of ADHESION SCIENCE and TECHNOLOGY
www.brill.nl/jast

Role of Vertical Component of Surface Tension of the Droplet on the Elastic Deformation of PDMS Membrane

Ying-Song Yu, Zhenyu Yang and Ya-Pu Zhao *

State Key Laboratory of Nonlinear Mechanics, Institute of Mechanics, Chinese Academy of Sciences, Beijing 100190, China

Received in final form 2 March 2008

Abstract

Poly(dimethylsiloxane) (PDMS) has been widely used in lab-on-a-chip and micro- total analysis systems (μ-TAS), thus wetting and electrowetting behaviors of PDMS are of great importance in these devices. PDMS is a kind of soft polymer material, so the elastic deformation of PDMS membrane by a droplet cannot be neglected due to the vertical component of the interfacial tension between the liquid and vapor, and this vertical component of liquid–vapor surface tension is also balanced by the stress distribution within the PDMS membrane. Such elastic deformation and stress distribution not only affect the exact measurement of contact angle, but also have influence on the micro-fluidic behavior of the devices. Using ANSYS code, we simulated numerically the elastic deformation and stress distribution of PDMS membrane on a rigid substrate due to the liquid–vapor surface tension. It is found that the vertical elastic deformation of the PDMS membrane is on the order of several tens of nanometers due to the application of a droplet with a diameter of 2.31 mm, which is no longer negligible for lab-on-a-chip and μ-TAS. The vertical elastic deformation increases with the thickness of the PDMS membrane, and there exists a saturated membrane thickness, regarded as a semi-infinite membrane thickness, and the vertical elastic deformation reaches a limiting value when the membrane thickness is equal to or thicker than such saturated thickness.

Keywords

Capillarity, wetting, Young's equation, vertical component, numerical simulation

1. Introduction

In his historic essay in 1805 [1], Thomas Young established the law of the contact angle in capillarity. He is quoted from his essay [1, 2]: "But it is necessary to premise one observation, which appears to be new, and which is equally consistent with theory and experiment; that is, for each combination of a solid and a fluid, there is an appropriate angle of contact between the surfaces of the fluid, exposed

* To whom correspondence should be addressed. Fax: +86-10-6256-1284; e-mail: yzhao@imech.ac.cn

 DOI:10.1163/156856108X305732

to the air, and to the solid". This, together with the Young–Laplace equation (relating the surface tension to the pressure and radius of curvature) have formed the foundations of Capillarity science and practice [2]. Now, capillarity has become an interdisciplinary science.

Thomas Young stated that when a drop of liquid makes contact with a planar, isotropic solid surface it will approach the contact line following a dihedral angle, ϕ, that depends on the solid and liquid surfaces according to his well-known equation of contact angle

$$\cos\phi = \frac{\gamma_{sv} - \gamma_{sl}}{\gamma_{lv}}, \tag{1}$$

which is the equilibrium of the horizontal forces as shown in the so-called 'Young's diagram' in Fig. 1. Here γ_{sv}, γ_{sl} and γ_{lv} are the interfacial tensions between solid–vapor, solid–liquid and liquid–vapor, respectively. Young asserted that the contact angle ϕ depends only on the material properties [3]. The equivalent equation, equation (1), was stated in algebraic form by Dupre in 1869 [4], along with the definition of work of adhesion [5], and sometimes equation (1) is also called the Young–Dupre equation [2].

One immediately notices from the Young diagram (Fig. 1) that the forces do NOT in general balance completely: a net force

$$\gamma_N = \gamma_{lv} \sin\phi, \tag{2}$$

appears normal to the smooth solid surface. Young wrote nothing about this component in equation (2) [3]. Hondros [2] pointed out three major shortcomings of the contact angle law in the practical applications in his memorial article in honor of Dr. Thomas Young on the occasion of the 200th anniversary of the presentation of his pivotal essay. In this article, Hondros wrote: "But probably the most questionable feature of the application of the Law is that a vertical component of surface tension, $\gamma_{lv} \sin\phi$ is ignored. In most cases this may be justified, but there are combinations of substances where it is suspected that the shape of the three-phase boundary could be affected because of the highly stressed zone of contact. This matter should be studied further".

As a matter of fact, many scientists have studied or commented on this problem. In 1875, Maxwell [6] commented: "The surface tensions normal to the surface are

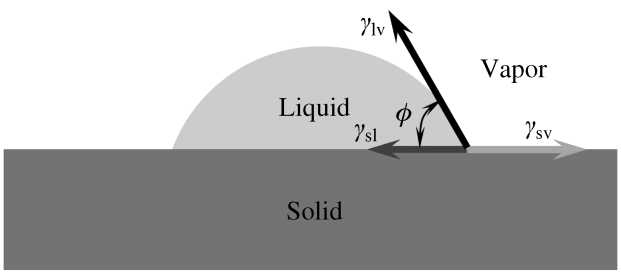

Figure 1. The Young diagram — a liquid droplet resting on a solid surface.

balanced by the resistance of the solid". In 1961, Lester [7] studied theoretically the contact angles of liquids at deformable solid surfaces. Madasu and Cairncross [8] presented a finite element formulation for predicting an elastic deformation, close to the static wetting line for a special case with conditions: contact angle $\phi = 90°$ and $\gamma_{sv} = \gamma_{sl}$. In 2003, de Gennes *et al.* commented in their book [9]: "The projection of the capillary forces onto the vertical axis is balanced out by a force of reaction exerted by the solid". Some researchers have studied the elastic deformation of thin plates [10–12] due to the droplet. Shanahan and co-workers [13–19] studied the spreading dynamics of a liquid drop on viscoelastic solids both theoretically and experimentally, and they reported a direct evidence for the wetting ridge obtained using scanning interferometric microscopy [15]; also they estimated of the height of the ridge pulled by the vertical component of the droplet [16] as:

$$h \approx \frac{\gamma_{lv} \sin \phi}{G}, \tag{3}$$

where G is the shear modulus of the soft solid. Extrand and Kumagai [20] performed some wetting experiments using soft rubber, and they found that a ridge was pulled up of the uncrosslinked butadiene rubber by the droplet and resulted in contact angle hysteresis of 69°.

The vertical component in the Young equation can be neglected for large structures unless the large structures experience surface deformation that influences wettability. Nevertheless, it may have practical applications in microelectromechanical systems (MEMS) and nanoelectromechanical systems (NEMS). Recently, some authors have exploited the bending of microcantilevers due to nanobubbles in water [21], capillary wrinkling of floating thin polymer films [22] and sessile-drop-induced bending of atomic force microscope cantilevers [23].

PDMS has been widely used as a base material in lab-on-a-chip and micro-total analysis systems (μ-TAS), so wetting and electrowetting behaviors of PDMS are of great concern in these devices [24, 25]. As a soft material, the PDMS with a sessile droplet may have relatively large elastic deformation due to the vertical component of the interfacial tension between liquid and vapor. To more precisely manipulate the liquid in lab-on-a-chip or μ-TAS, we have to estimate the amount of vertical elastic deformation as well as the stress distribution of the PDMS membrane due to the sessile droplet. Using commercial ANSYS code, we simulated the elastic deformation normal to the PDMS surface and the stress distribution within the PDMS membrane due to the liquid–vapor surface tension. We hope that this study will assist in a better design of the wetting and electrowetting behaviors of lab-on-a-chip and μ-TAS by using soft polymer materials.

2. Problem Formulation

Consider the contact of a droplet on an isotropic deformable PDMS membrane with a rigid substrate as shown in Fig. 2. Without loss of generality, the droplet is supposed to be spherical and the contact area with PDMS is a circle with the

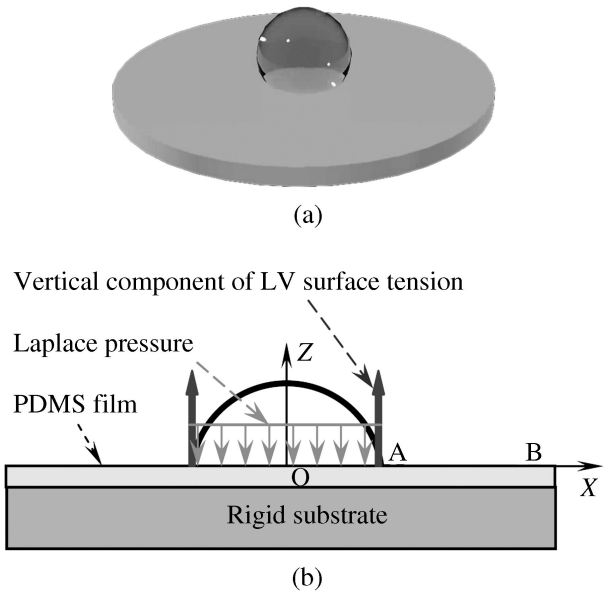

Figure 2. (a) Sketch of a water droplet on PDMS membrane. (b) Wetting equilibrium.

radius $a = 1.0$ mm. PDMS is a hydrophobic material, and the water contact angle is between $\phi = 108°$–$128°$ [24, 25], and is taken as $\phi = 120°$ for simplicity in the numerical calculation in the present paper. The diameter of the droplet is thus $d = 2a/\sin(2\pi/3) \cong 2.31$ mm. The surface tension of water is $\gamma_{\mathrm{lv}} = 72 \times 10^{-3}$ N/m at 25°C [26]. The weight of the liquid droplet can be neglected since the diameter of the droplet is less than the capillary length for water which is approximately $l_{\mathrm{Capillary}} = \sqrt{\gamma_{\mathrm{lv}}/\rho g} \cong 2.7$ mm, here ρ and g are the mass density of water and gravitational acceleration, respectively. It is supposed that there is no relative motion between the PDMS membrane and the rigid substrate.

For the first-order approximation, the elastic deformation of the PDMS induced by the vertical component of the surface tension of the droplet is supposed to be small enough, so PDMS material can be regarded as a linear elastic material for small elastic deformation with sufficient accuracy. The Young's modulus of PDMS is 360–870 kPa [27].

As shown in Fig. 2, the wetted area is

$$A = \pi a^2 = \pi\left(R \sin\frac{2\pi}{3}\right)^2 = \frac{3\pi}{4}R^2, \tag{4}$$

where $R = d/2$ is the radius of curvature of the droplet. The Young–Laplace pressure is

$$P = 2\frac{\gamma_{\mathrm{lv}}}{R} = 2\frac{\gamma_{\mathrm{lv}}}{a}\sin\phi. \tag{5}$$

The Young–Laplace pressure in equation (5) acts on the wetted area [7, 23] and is compensated by the vertical component of the surface tension in equation (2).

3. Simulation Procedure, Results and Analysis

A commercial ANSYS 10.0 package was used to solve this problem. Actually, PDMS is a kind of Mooney–Rivlin rubber-like material with incompressible property. But for the small deformation, the PDMS membrane can also be reasonably regarded as a linear elastic material. Hence, Poisson's ratio of 0.499 [27] was used in the following calculation, which made the material approximately incompressible. Figure 3 shows the central symmetric mesh for the finite element model using ANSYS. For the finite element model, the radius of the PDMS membrane was 10 mm and the diameter of the water droplet was 2.31 mm as shown in Fig. 2a. The PDMS membrane thickness varied from 0.5 mm to 10.0 mm. The thicknesses of 0.5 mm and 10.0 mm consist of 1920 eight-node solid elements with 2709 nodes and 12 000 eight-node solid elements with 15 351 nodes, respectively. Fine elements with a radius of 1.0 mm were added on the surface of the PDMS in order to resolve the droplet acting on the PDMS, as shown in the lower right corner of Fig. 3.

The boundary conditions are presented in Fig. 2b. The nodes on the axis of symmetry of the PDMS membrane cannot move in the radial direction. Likewise the nodes on the bottom of the membrane cannot move in all directions because the PDMS membrane is considered to perfectly adhere to the substrate. The Young–Laplace pressure was considered to be a uniform pressure acting in the contact

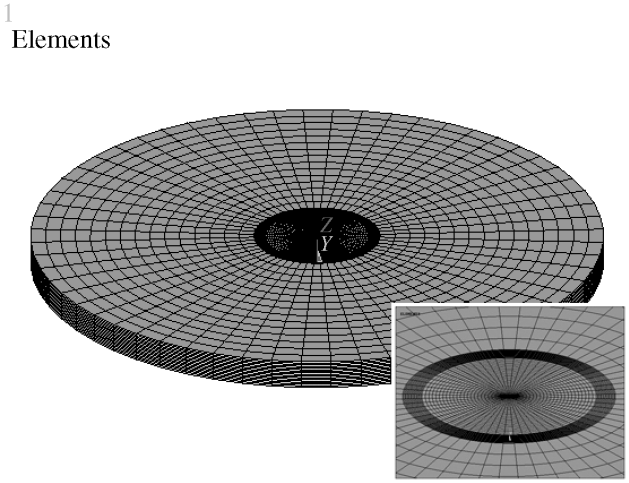

Figure 3. Mesh of the finite element model used. The center region of the mesh is amplified in the lower right corner.

region with a radius of 1.0 mm and the pressure was averagely transformed to concentrate forces on the nodes. The vertical component of liquid–vapor surface tension was reduced to a uniform force acting on the contour of the circular contact region. All the nodes on the contour were equidistant and the vertical component was averagely distributed to these nodes. In this paper, the deformation of the water droplet was not taken into account.

Figure 4a presents the vertical displacement of the line O–A–B (Fig. 2a) on the PDMS membrane. In the region where the water droplet contacts the PDMS, the value of vertical displacement increases with the thickness of the PDMS membrane. When the thickness increases, the vertical displacement reaches a limit of about 2.0 mm. It can be deduced that there exists a saturated membrane thickness about 2.0 mm, which can be regarded as a semi-infinite membrane thickness. As shown in Fig. 4b, the vertical displacement at point A decreases with the increase of the Young's modulus of the PDMS membrane. The PDMS membrane with Young's modulus of 360 kPa shows the maximum displacement, which converges to a limiting value of about 0.321 μm. For the PDMS membranes with Young's moduli of 500 kPa and 740 kPa, the limiting values are about 0.231 μm and 0.156 μm, respectively. In Ref. [16], the authors estimated the vertical displacement of the ridge using equation (3) as: $h \approx \gamma_{\mathrm{lv}} \sin\phi / G \approx 0.253$ μm for $E = 740$ kPa, while in our calculation, the value is approximately 0.156 μm using the same material constants. Therefore, numerical simulation is indeed necessary to obtain detailed information on the elastic deformation of the ridge. The nephogram of displacement in the normal direction is given in Fig. 5. (Nephogram: The value of a certain small region in a field (e.g. stress or displacement) is marked by a corresponding color. When the values are not equal everywhere, the field can be converted to a multi-color map, which is called nephogram.) The red region identifies the region with the maximum vertical displacement. The vertical component of the liquid–vapor surface tension produces tensile stress in this region. And the blue region for the minimum displacement is where the Young–Laplace pressure is applied and induces compressive stress. The amplitude of the vertical displacement has been magnified for convenient observation.

The von Mises stress is taken as the equivalent stress σ_{E}, which is computed as:

$$\sigma_{\mathrm{E}} = \sqrt{\frac{(\sigma_1 - \sigma_2)^2 + (\sigma_2 - \sigma_3)^2 + (\sigma_3 - \sigma_1)^2}{2}}, \tag{6}$$

where σ_1, σ_2 and σ_3 are the principal stresses. The equivalent stress distribution along the line O–A–B (see Fig. 2b) is shown in detail in Fig. 6. In the contact region, the equivalent stress distribution along the line O–A–B indicates that the membrane thickness affects the stress. The maximum stress is present at the point A ($x = 1.0$ mm) (Fig. 6a), where the vertical component of the liquid–vapor surface tension is applied to the PDMS membrane. More details about the

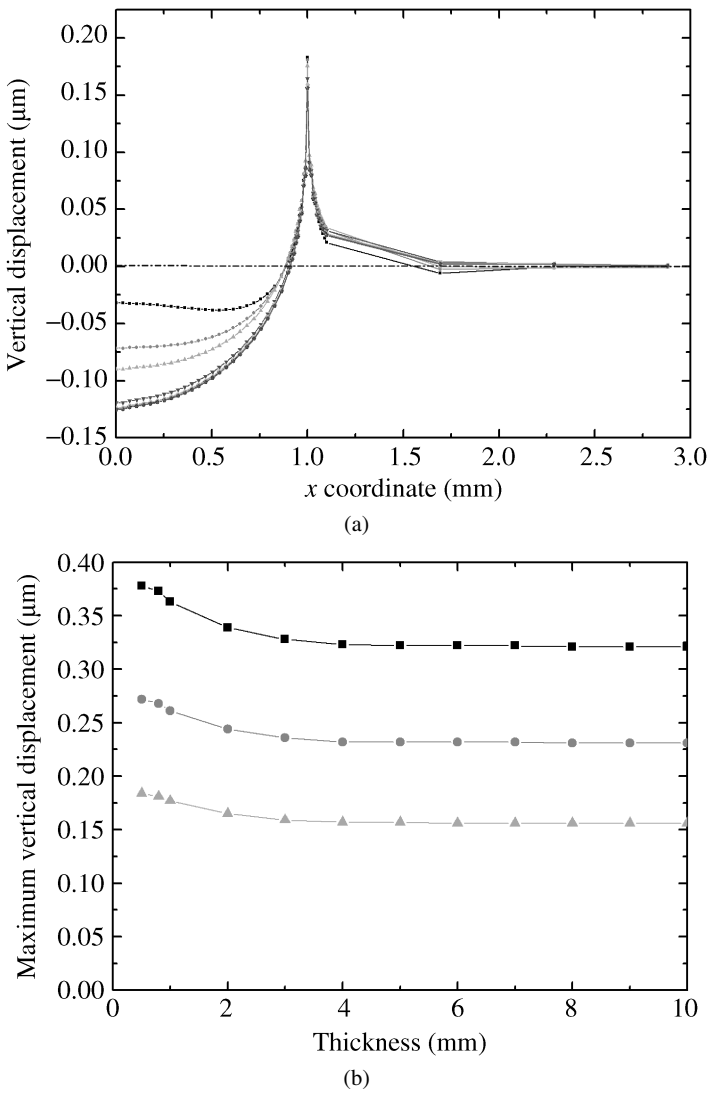

Figure 4. (a) Vertical displacement distribution along the line O–A–B (see Fig. 2b) with PDMS membrane thickness varying from 0.5 mm to 10.0 mm (— ▪ — 0.5 mm, — ● — 0.8 mm, — ▲ — 1.0 mm, — ▼ — 2.0 mm, — ◆ — 3.0 mm, — ◀ — 4.0 mm, — ▶ — 5.0 mm, — ● — 6.0 mm, — ★ — 7.0 mm, — ● — 8.0 mm, — ● — 9.0 mm and — + — 10.0 mm). (b) Maximum vertical displacement at point A changes with Young's modulus of the PDMS membrane (— ■ — $E = 360$ kPa, — ● — $E = 500$ kPa and — ▲ — $E = 740$ kPa).

equivalent stress in the contact region are shown in Fig. 6b, which shows that the equivalent stress in the contact region varies non-linearly with the x coordinate. For the PDMS membrane with a thickness 0.5 mm, the equivalent stress in the contact region reduces with the x coordinate and then increases. The decline region of the stress is a convex curve. For the other PDMS membranes with dif-

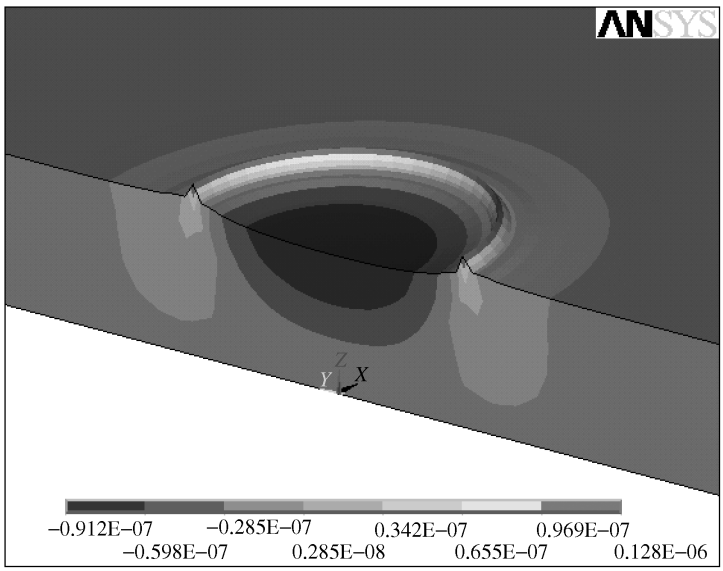

Figure 5. Nephogram of the vertical displacement distribution.

ferent thicknesses, the stresses also show a similar trend. But when the thickness is larger than 2.0 mm, the curve of the stress distribution *versus x* coordinate is concave. With the increase of the thickness of the PDMS membrane, the maximum stress at the point A decreases and converges to a limiting value of about 1106 Pa (Fig. 6c). As shown in Fig. 6d, the Young's modulus of the PDMS membrane has no influence on the equivalent stress. The nephogram of equivalent stress in the PDMS membrane is shown in Fig. 7 with the vertical displacement magnified. The values of the stresses are identified by the colored contour legend, as shown in the lower part of Fig. 7. The red region is the region where the vertical component of liquid–vapor surface tension is applied and shows the maximum stress.

4. Conclusion

The elastic deformation of the PDMS membrane, which is produced by the normal component of liquid–vapor surface tension of the droplet resting on the PDMS membrane, is calculated using FEM and analyzed. It is found that the vertical elastic deformation of the PDMS membrane is on the order of several tens of nanometers due to the application of a droplet with a diameter of 2.31 mm, which is no longer negligible for lab-on-a-chip and μ-TAS. A saturated membrane thickness of about 2.0 mm can be reasonably regarded as a semi-infinite membrane thickness.

Detailed distributions of vertical elastic deformation and equivalent stress are presented in this paper. The vertical elastic deformation decreases with increasing

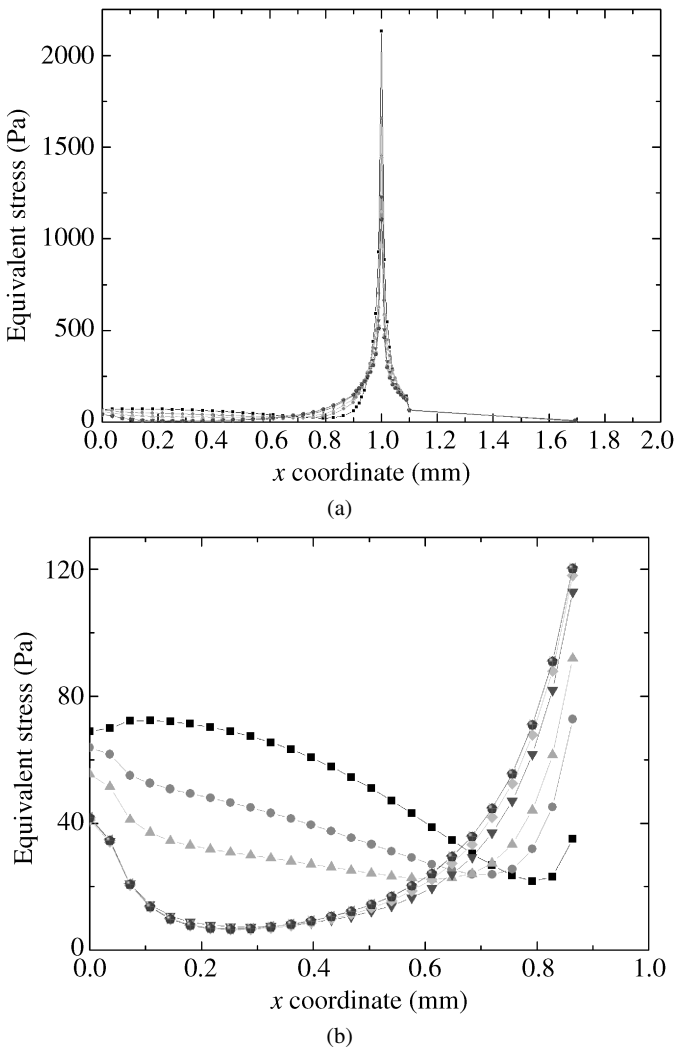

Figure 6. (a) Equivalent stress distribution along the line O–A–B (see Fig. 2b) with PDMS membrane thickness varying from 0.5 mm to 10.0 mm (— ■ — 0.5 mm, — ● — 0.8 mm, — ▲ — 1.0 mm, — ▼ — 2.0 mm, — ◆ — 3.0 mm, — ◀ — 4.0 mm, — ▶ — 5.0 mm, — ● — 6.0 mm, — ★ — 7.0 mm, — ● — 8.0 mm, — ● — 9.0 mm and — + — 10.0 mm). (b) Magnified view of the equivalent stress distribution in the contact region with thickness varying from 0.5 mm to 10.0 mm (— ■ — 0.5 mm, — ● — 0.8 mm, — ▲ — 1.0 mm, — ▼ — 2.0 mm, — ◆ — 3.0 mm, — ◀ — 4.0 mm, — ▶ — 5.0 mm, — ⬢ — 6.0 mm, — ★ — 7.0 mm, — ⬟ — 8.0 mm, — ● — 9.0 mm and — + — 10.0 mm). (c) Magnified view of the equivalent stress distribution near point A (see Fig. 2b) with PDMS membrane thickness varying from 0.5 mm to 10.0 mm (— ■ — 0.5 mm, — ● — 0.8 mm, — ▲ — 1.0 mm, — ▼ — 2.0 mm, — ◆ — 3.0 mm, — ◀ — 4.0 mm, — ▶ — 5.0 mm, — ● — 6.0 mm, — ★ — 7.0 mm, — ● — 8.0 mm, — ● — 9.0 mm and — + — 10.0 mm). (d) Equivalent stress at point A (see Fig. 2b) with Young's modulus (360 kPa, 500 kPa and 740 kPa) of PDMS membrane (— ■ — $E = 360$ kPa, — ● — $E = 500$ kPa and — ▲ — $E = 740$ kPa).

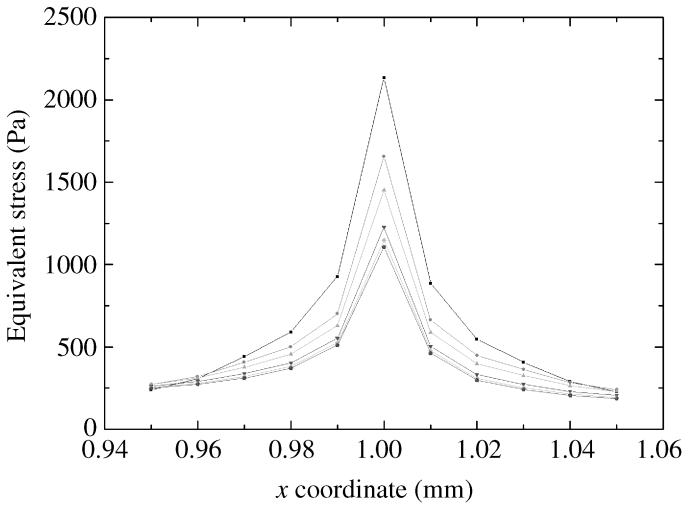

(c)

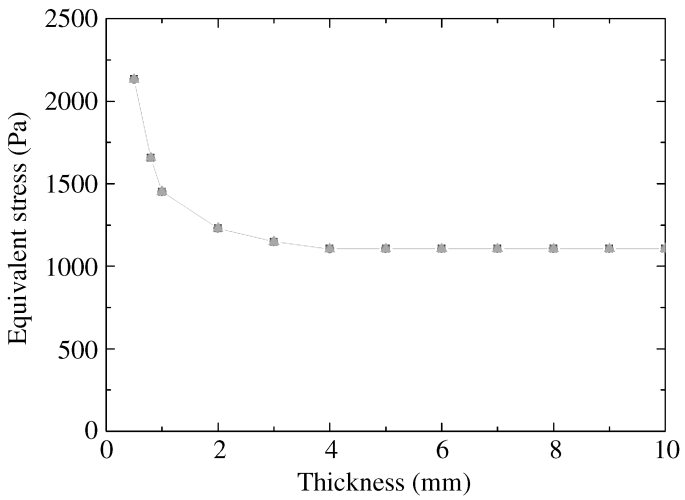

(d)

Figure 6. (Continued.)

Young's modulus. The Young's modulus of the PDMS membrane has no influence on the equivalent stress.

Acknowledgements

This work was jointly supported by the National Basic Research Program of China (973 Program, Grant No. 2007CB310500) and the National Natural Science Foundation of China (NSFC, Grant Nos 10772180 and 10721202).

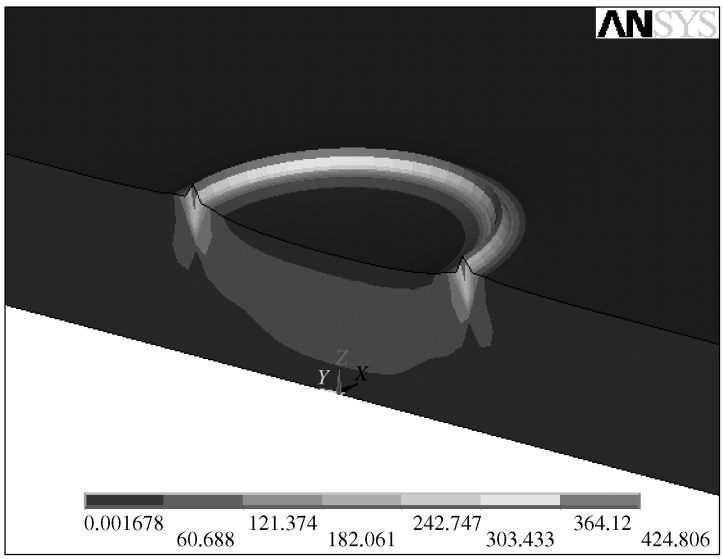

Figure 7. Nephogram of the equivalent stress distribution.

References

1. T. Young, *Philos. Trans. R. Soc. London* **95**, 65 (1805).
2. E. D. Hondros, *J. Mater. Sci.* **40**, 2119 (2005).
3. R. Finn, *Phys. Fluids* **18**, 047102 (2006).
4. A. Dupre, *Theorie Mecanique de la Chaleur*. Gauthier-Villars, Paris (1869).
5. A. W. Adamson, *Physical Chemistry of Surfaces*, 6th ed. Wiley, New York, NY (1997).
6. J. C. Maxwell, in: *Encyclopedia Britannica*, 9th ed. Samuel L. Hall, New York, NY (1875).
7. G. R. Lester, *J. Colloid Sci.* **16**, 315 (1961).
8. S. Madasu and R. A. Cairncross, *Int. J. Numer. Mech. Fluids* **45**, 301 (2004).
9. P.-G. de Gennes, F. Brochard-Wyart and D. Quere, *Capillarity and Wetting Phenomena*. Springer, New York, NY (2004).
10. M. A. Fortes, *J. Colloid Interface Sci.* **100**, 17 (1984).
11. J. Olives, *J. Phys.-Condens. Matter* **5**, 2081 (1993).
12. R. Kern and P. Müller, *Surface Sci.* **264**, 467 (1992).
13. A. Carré and M. E. R. Shanahan, *Langmuir* **11**, 24 (1995).
14. A. Carré and M. E. R. Shanahan, *Langmuir* **11**, 1396 (1995).
15. A. Carré, J. C. Gastel and M. E. R. Shanahan, *Nature* **379**, 432 (1996).
16. M. E. R. Shanahan and A. Carré, *Colloids Surfaces A* **206**, 115 (2002).
17. M. E. R. Shanahan, *J. Phys. D: Appl. Phys.* **21**, 981 (1988).
18. M. E. R. Shanahan and A. Carré, *J. Adhesion* **57**, 179 (1996).
19. M. E. R. Shanahan and A. Carré, in: *Mittal Festschrift on Adhesion Science and Technology*, W. J. van Ooij and H. R. Anderson Jr (Eds), p. 239. VSP, Utrecht, The Netherlands (1998).
20. C. W. Extrand and Y. Kumagai, *J. Colloid Interface Sci*. **184**, 191 (1996).
21. S. M. Jeon, R. Desikan, F. Tian and T. Thundat, *Appl. Phys. Lett.* **88**, 103118 (2006).
22. J. Huang, M. Juszkiewicz, W. H. de Jeu, E. Cerda, T. Emrick, N. Menon and T. P. Russell, *Science* **317**, 650 (2007).

23. T. Haschke, E. Bonaccurso, H. J. Butt, D. Lautenschlager, F. Schonfeld and W. Wiechert, *J. Micromech. Microeng.* **16**, 2273 (2006).
24. J. T. Feng and Y. P. Zhao, *Biomed. Microdevices* **10**, 65 (2008).
25. W. Dai and Y. P. Zhao, *Int. J. Nonlinear Sci. Numer. Simul.* **8**, 519 (2007).
26. http://hyperphysics.phy-astr.gsu.edu/hbase/surten.html
27. D. Armani and C. Liu, in: *Proc. 12th Intl. Conf. on MEMS (MEMS'99)*, p. 222. Orlando, FL, USA (1999).